FIRING STABILITY OF SiN_y / SiN_x SURFACE PASSIVATION STACKS FOR CRYSTALLINE SILICON SOLAR CELLS

S. Gatz[1], F. Einsele[2], T. Dullweber[1], R. Brendel[1,3]
[1] Institute for Solar Energy Research Hamelin (ISFH), Am Ohrberg 1, D-31860 Emmerthal, Germany
[2] Institute for Energy Research (IEF-5), Forschungszentrum Jülich, Leo-Brandt-Straße, D-52428 Jülich, Germany
[3] Department of Solar Energy, Institute of Solid-State Physics, Leibniz University at Hannover, Appelstrasse 2, D-30167 Hannover, Germany

ABSTRACT: In this study, we investigate amorphous silicon nitride passivation stacks in order to combine the excellent surface passivation of amorphous silicon with the excellent firing stability of silicon nitride layers. Structural and lifetime investigations show that these stacks provide an excellent surface passivation quality after a firing step with effective surface recombination velocities of (5.2 ± 2) cm/s on *p*-type (1.5 Ωcm) FZ-silicon wafers at an injection density $\Delta n = 10^{15}$ cm^{-3}. The increased bonding strength of hydrogen in the amorphous silicon nitride network is confirmed by hydrogen effusion measurements. Moreover the beneficial effect by a silicon nitride capping layer is underlined. We apply these passivation stacks to the rear of solar cells using *p*-type boron-doped Cz- and FZ-silicon wafers. After local laser ablation of the dielectrics and full-area metallization of the rear we achieve energy conversion efficiencies up to 19.4 % on laboratory-type solar cells and 18.3 % on industrial-type solar cells with screen-printed contacts compared to reference solar cells with conventional aluminum back surface field showing 17.9 %.

Keywords: surface passivation, PERC solar cell, silicon nitride

1 INTRODUCTION

Currently, highly efficient PERC (passivated emitter and rear cell) solar cells [1] are intensively investigated by research institutes and companies. As a key process step, the high-throughput plasma-enhanced chemical vapor deposition (PECVD) for the deposition of the rear passivation layer is an attractive technique due to its opportunities for cost savings. For an industrial application, there are three main requirements for the rear passivation layers:

- Excellent surface passivation quality after the high-temperature co-firing step
- No parasitic shunting [2] at the contacts
- Improved internal reflectance at the rear

Silicon nitride (SiN_x) layers provide an excellent surface passivation quality [3]. The passivation quality and firing stability depends strongly on the refractive index of the passivation layer [3,4]. A refractive index of $n \approx 2.4$ results in low effective surface recombination velocities S_{eff} for the as deposited state, whereas a layer with $n \approx 2.05$ performs best after a firing step ($T = 800...900$ °C) [5]. The latter configuration is e.g. used for conventional screen-printed solar cells to passivate the phosphorous-diffused emitter at the front. The passivation of these SiN_x films deposited in an NH_3-rich gas mixture relies primarily on the field effect passivation provided by a high density of fixed positive charges in the insulating SiN_x films. Secondly, the surfaces are passivated by atomic hydrogen (H) released from the precursor gases during the PECVD deposition. However, parasitic shunting between the back contacts and the inversion layer underneath the SiN_x interface was found to deteriorate the cell performance for *p*-type substrates [2].

In contrast, intrinsic amorphous silicon (a-Si) films deposited on crystalline Si exhibit, if any, only small fixed charge densities and therefore do not cause parasitic shunting [2]. These films provide the same low S_{eff} values as thermally grown SiO_2 [6,7,8,9,10], because atomic hydrogen (H) is released during PECVD deposition. It saturates the dangling bonds at the interface, and thereby decreases the interface state density [11]. However, during the high-temperature co-firing step the surface passivation quality degrades significantly. Plagwitz et al. [7] and Ulyashin et al. [12] showed that depositing a SiN_x capping layer with $n_{SiN} \approx 2.05$ on top not only protects the a-Si layer from the aluminum (Al) metallization but also improves the thermal stability of the surface passivation. By optimization of the SiN_x deposition, an enhanced thermal stability of these films is achieved [13]. However, the a-Si / SiN_x stacks were only shown to be stable for firing at $T < 750$°C, thus requiring special low temperature metallization pastes. Applying standard pastes with firing temperatures of around 800°C the surface passivation deteriorates severely. Stack systems based on amorphous silicon oxide (SiO_x) and SiN_x demonstrated an S_{eff} below 60 cm/s after a high-temperature firing step [14,15]. A double layer of amorphous silicon-rich oxynitride capped with SiN_x showed a good passivation quality and a good thermal stability during firing [16].

In this paper, we investigate silicon nitride passivation stacks (SiN_y / SiN_x) with silicon-rich SiN_y and an SiN_x capping layer. This approach combines the surface passivation properties of a-Si with the superior firing stability of silicon nitride SiN_x layers. The main idea is to increase the thermal stability of the surface passivation by supplying minor amounts of NH_3 during the PECVD deposition in order to reduce hydrogen effusion during a conventional screen-printing firing process. Moreover, it is known that the positive fixed charge density, responsible for the parasitic shunting, is strongly reduced compared to SiN_x if the N content in the amorphous film is low [17,18].

2 EXPERIMENTAL

2.1 Test sample preparation and measurement techniques

In this study, FTIR measurements, Hydrogen (H) effusion and lifetime investigations are performed using 290 µm-thick *p*-type boron-doped 1.5 Ωcm, shiny etched Float-Zone (FZ) silicon wafers. The 10 nm-thick SiN_y passivation layers are deposited by a direct plasma PECVD system. Immediately before the SiN_y deposition, the FZ wafers are cleaned in a wet chemical RCA process. PECVD-deposition parameters as temperature, plasma power, pressure and total gas flow remain constant during the experiments. The composition of the SiN_y passivation layer is modified by varying the NH_3-content in the $SiH_4/NH_3/H_2$ gas mixture. As shown in Fig. 1, the 100-200 nm thick SiN_x capping layer is deposited on top of the passivation layer by an inline microwave PECVD system.

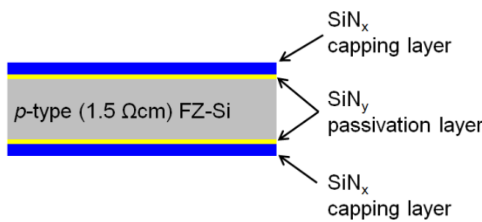

Figure 1: *Schematic drawing of the samples prepared for the hydrogen effusion and QSSPC measurements. The FZ-silicon surfaces are symmetrically passivated by a* SiN_y */* SiN_x *stack.*

For comparison we deposit also amorphous silicon nitride single layers with refractive indices ranging from 1.9 to 3.1 by a remote plasma PECVD system with varying the SiH_4-content in the $SiH_4/NH_3/H_2$ gas mixture. To determine the effective surface recombination velocity S_{eff} after a firing step, symmetrical SiN_y / SiN_x passivated 290 µm-thick FZ silicon wafers pass through a belt furnace with 830°C set peak temperature and 3 m/min belt velocity. The dwell time at the peak temperature is approximately 5 seconds.

The real part of the refractive index *n* of the dielectric films is measured by a monochromatic (λ = 632.8 nm) ellipsometer (Plasmos). Therefore, single layers with comparably high NH_3/SiH_4 ratio in the PECVD gas mixture are deposited on shiny etched FZ-Si wafers ($n_{Si\text{-}wafer}$ = 3.87). Decreasing the NH_3-content in the gas mixture and therefore increasing the silicon content in the dielectric layer results in an increased refractive index. That exceeds therefore the limit in accuracy of the monochromatic ellipsometry when the PECVD layer is deposited on a crystalline silicon wafer. Therefore, single layers with a low NH_3/SiH_4 ratio in the PECVD gas mixture are deposited on 1.1 mm-thick BOROFLOAT® glass with a refractive index n_{glass} = 1.46. InfraRed (IR) absorption measurements were performed on a Bruker Equinox 55 Fourier transform IR Spectrometer (FTIR) using a mid IR source and a DTGS detector. The FTIR spectra are recorded at wavenumbers ranging from 5000 to 200 cm^{-1} with a resolution of 4 cm^{-1}.

Hydrogen effusion experiments reveal information on the thermal stability of H-bonds in SiN_y single and SiN_y / SiN_x double layers. Thereby our samples are annealed with a heating rate of 20 K/min in vacuum. By means of a mass spectrograph we detect out-diffused H atoms and molecules in real time. From literature it is well known that for amorphous silicon a particular H effusion peak at a characteristic temperature T_{eff} is a measure of the thermal stability of the H in the a-Si:H layer. Details about the measurement technique are described elsewhere [19].

To determine the surface passivation quality, we measure the effective lifetime τ_{eff} of symmetrically passivated *p*-type FZ-Si wafers by means of the quasi-steady state photoconductance (QSSPC) method [20,21]. By attributing the total measured recombination rate including the recombination in the silicon bulk to the interface, we estimate the upper limit for the effective surface recombination velocity

$$S_{eff} = \frac{W}{2 \cdot \tau_{eff}} \quad (1)$$

from τ_{eff} and the wafer thickness *W*.

2.2 PERC solar cell processing

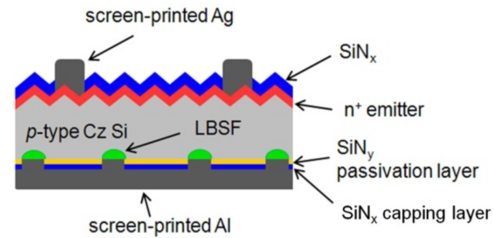

Figure 2: *Schematic drawing of the screen-printed PERC solar cell with local openings in the* SiN_y */* SiN_x *passivation stack.*

We apply the SiN_y / SiN_x surface passivation to the rear of PERC solar cells using 200 µm-thick Czochralski-grown *(100)*-oriented, boron-doped 2 to 3 Ωcm pseudo-square silicon wafers. A schematic drawing is shown in Fig. 2. In the solar cell process a protective coating on the rear allows for a single side texturing and phosphorus diffusion using $POCl_3$. The sheet resistance is (65±10) Ω/□ measured by a 4-point probe method. After removal of the phosphosilicate glass and the dielectric at the rear by a HF etch, the rear surface is passivated by a PECVD SiN_y / SiN_x stack as described in section 2.1. The phosphorus emitter at the front side receives a conventional SiN_x anti reflection coating deposited by PECVD technique. The SiN_y / SiN_x rear stack is locally ablated by a laser with pulse lengths of 10 picoseconds and a wavelength of 532 nm. The screen-printed contacts to the emitter and to the base are formed by Ag and Al pastes, respectively. Each print process is completed by a 5 minute drying process at about 200°C. The local Al-BSF (LBSF) forms during the co-firing step in a belt furnace with a set peak temperature of 870 °C and a belt velocity of 3 m/min. The metallization fraction at the rear *f* is 16%. Solar cells with a conventional full-area Al-BSF are also manufactured for reference purposes. We apply laser edge isolation. The solar cell area is 141 cm^2.

Moreover, we fabricate laboratory-type PERC solar cells based on B-doped 0.5 Ωcm FZ-Si wafers. Thereby, the front and the rear contacts are realized by evaporated Al. The phosphorus-doped emitter is passivated by an a-Si / SiN_x passivation stack. The solar cell area is 4 cm^2.

3 RESULTS AND DISCUSSION

3.1 FTIR measurements

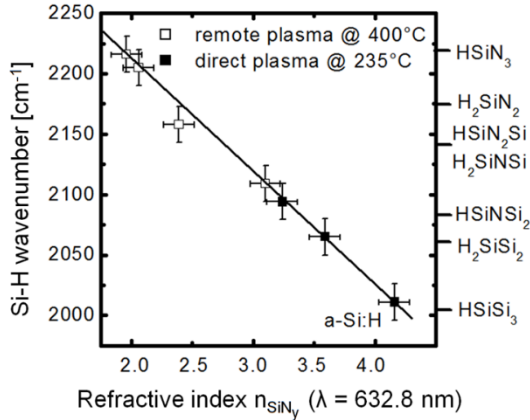

Figure 3: *Wavenumber of the Si-H peak position versus the real part of the refractive index for various silicon nitride single layers obtained by FTIR spectroscopy. The insertions on the right hand side correspond to the peak position of several Si-H absorption peaks [22]. The higher the refractive index the less nitrogen is back-bonded to silicon-hydrogen connections. The line is a guide to the eye.*

In order to characterize the passivation mechanism of the SiN_y layers, FTIR absorption measurements of SiN_y passivated silicon wafers are performed. Fig. 3 shows the Si-H bond absorption peak position as a function of the refractive index. The Si-H peak position wavenumber shifts linearly from 2220 cm^{-1} to 2015 cm^{-1} with increased real part of the refractive index n (from 1.90 to 4.16). This holds independently of the used PECVD deposition systems. With increasing index of refraction, the number of Si-N back-bonds decreases, while the concentration of Si-H bonds increases [22]. The shift of the Si-H peak to higher wavenumbers for a decreasing refractive index corresponds to an increase of the Si-H binding energy and therefore to an increase of the thermal H stability in the layers with decreased refractive index.

3.2 Hydrogen effusion

In SiN_y / SiN_x stacks, hydrogen is bonded in an amorphous silicon nitride network. Thermally stimulated H diffuses out of the PECVD layers, and is therefore no longer available to passivate the silicon surface. This evolution can be shown by H effusion experiments [19]. Fig. 4 shows examples of the measured effusion rate for different passivation layers. The H effusion rate of an a-Si:H single layer starts to increase at temperatures of about 300°C and exhibits a peak at a characteristic effusion temperature T_{eff} of nearly 500°C. For the SiN_y single layer with n_{SiN} = 3.6 both, the temperature at which effusion starts and the value of T_{eff} increase. By depositing a 100 nm-thick SiN_x capping layer on top of the SiN_y layer, the shoulder in the effusion rate at T_{eff} of around 630°C is attributed to the out-diffusion of H from the SiN_y passivation layer. The effusion peaks at temperatures of approximately 800°C and 1000°C are typical for the SiN_x capping layers with n_{SiN} = 2.05.

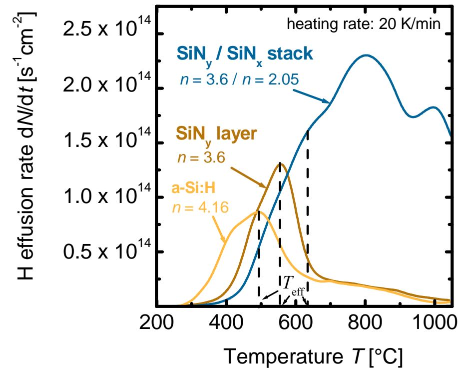

Figure 4: *Hydrogen effusion rate as a function of the actually measured temperature. The characteristic effusion temperatures T_{eff} are related to the respective maximal hydrogen effusion rate from the passivating film.*

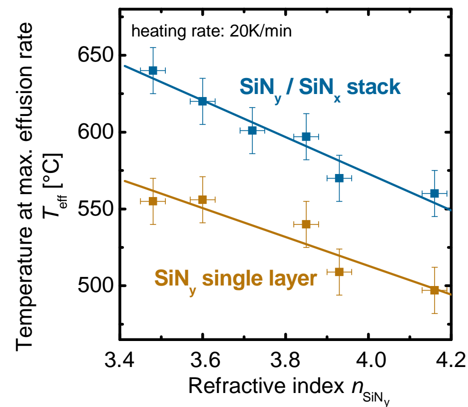

Figure 5: *Effusion temperatures T_{eff} from the SiN_y passivation layer depending on the refractive index n_{SiN} for both, SiN_y single and SiN_y / SiN_x stack layers, T_{eff} increases with decreasing n_{SiN}. The increase of T_{eff} using a SiN_x capping layer indicates the further reduction of hydrogen effusion.*

Fig. 5 shows the dependence of T_{eff} for effusion measurements of passivation layers from the real part of the refractive index n_{SiN} of the passivation layer. T_{eff} increases continuously from 500°C for an amorphous silicon single layer a-Si:H (n = 4.16) to about 550°C for SiN_y single layers with n = 3.48. Possibly, the out-diffusion of H is reduced because of the presence of nitrogen. From FTIR measurements in Fig. 3 we conclude that this is due to a stronger bonding strength of H to the Si-N network compared to the bonding strength to pure amorphous silicon network. In addition, Fig. 5 shows that T_{eff} increases about 60-90°C for all SiN_y layers, if a SiN_x capping layer is deposited on top of the SiN_y passivation layer. The reduced H effusion rate by a SiN_x capping layer agrees with previous investigations on a-Si / SiN_x layers [13].

3.3 Surface passivation quality

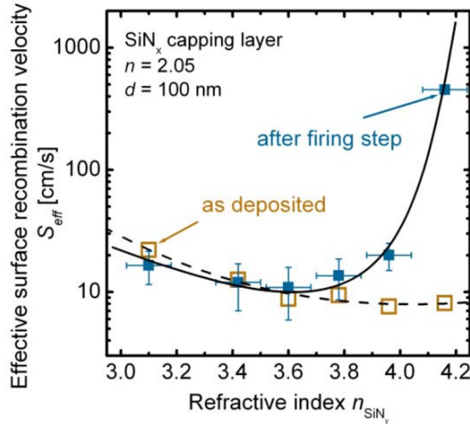

Figure 6: *Effective surface recombination velocity S_{eff} at $\Delta n = 10^{15}\ cm^{-3}$ before and after a firing step as a function of the passivation layer's refractive index n for SiN_y / SiN_x stacked layers. The lines are guides to the eye*

As shown in Fig. 6 the investigated PECVD SiN_y / SiN_x stacks provide an excellent surface passivation quality both before and after a firing step. In the as-deposited state the upper limit of the effective surface recombination velocity S_{eff} increases slightly from about 8 cm/s for the a-Si (n = 4.16) / SiN passivated wafer to above 20 cm/s for a SiN_y (n_{SiN} = 3.1) / SiN_x passivated wafer. However, the firing step with a set peak temperature of 900°C alters the S_{eff} dependence significantly. There is a minimum in S_{eff} depending on the refractive index in the range of n = 3.4 to 3.8 with S_{eff} = (12 ± 4) cm/s for stacks with n = 3.6. By further improvements in the PECVD process, we obtain S_{eff} = (5.2 ± 2) cm/s after the firing step. Increasing the refractive index further towards $n_{a\text{-}Si}$ = 4.16, S_{eff} increases strongly to well above 100 cm/s. We attribute the excellent firing stability to an increased bond strength of hydrogen in the SiN_y network as demonstrated by H effusion and FTIR measurements.

3.4 Cell results

Table 1 Solar cell parameters measured under standard testing conditions using *p*-type boron doped silicon.

No.	Si - wafer	Area [cm²]	Rear config.	Al rear metalliz.	V_{oc} [mV]	J_{sc} [mA/cm²]	*FF* [%]	η [%]
1	Cz, 1.5 Ωcm	141	SiN_y / SiN_x	screen-printed	633	37.1	77.8	18.3
2	Cz, 1.5 Ωcm	141	Al-BSF	screen-printed	628	36.3	78.2	17.9
3	FZ, 0.5 Ωcm	4	SiN_y / SiN_x	evapo-rated	665	37.4	78.1	19.4

Table 1 shows the resulting current-voltage parameters for a solar cell with SiN_y / SiN_x rear passivation (No. 1) compared to a reference cell with full-area aluminum BSF (No. 2). The PERC solar cell shows an improved (+ 0.8 mA/cm²) short circuit current density J_{sc} = 37.1 mA/cm² and an improved (+ 5 mV) open circuit voltage V_{oc} = 633 mV compared to the reference cell. In summary, the SiN_y / SiN_x rear passivation results in an energy conversion efficiency η of 18.3 % which is an improvement of 0.4 % in comparison to the reference solar cell with a full-area Al-BSF. Laboratory-type PERC solar cells based on FZ-Si (No. 3 in Tab. 1) shows with an energy conversion efficiency η of 19.4 % and an open circuit voltage of 665 mV the high potential of the SiN_y / SiN_x passivation stack.

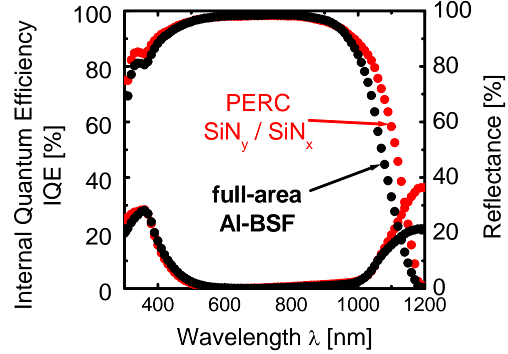

Figure 7: *Internal quantum efficiency (IQE) and reflectance of solar cells with SiN_y / SiN_x passivated rear side (red, No. 1 in Tab.1) and a full-area Al-BSF (black, No. 2 in Tab.1).*

In Fig. 7, the internal quantum efficiency (IQE) and reflectance of a solar cell (No. 1 of Tab.1) with SiN_y / SiN_x rear side passivation stack is shown as a function of the wavelength. For comparison, data for a solar cell with a full-area Al-BSF are included (No. 2 of Tab.1). Using an IQE evaluation program from Fischer [23], based on models by Basore [24] and Brendel et al. [25], we extract the effective rear surface recombination velocity $S_{eff,rear}$ from the measured IQE data in the wavelength region from 850 nm to 1000 nm. We compare measured data with simulations considering the accuracy of measurements. The solar cell with SiN_y / SiN_x rear side passivation has an $S_{eff,rear}$ of (400 ± 100) cm/s. That value is slightly smaller than $S_{eff,rear}$ of the solar cell with full-area Al-BSF of about (550 ± 100) cm/s, showing the improved surface passivation quality by the SiN_y / SiN_x stack. However, assuming 600 cm/s for local Al contacts, $S_{eff,rear}$ = 400 cm/s corresponds to a surface recombination velocity of about 300 cm/s in the passivated areas [26]. That value clearly exceeds the S_{eff} = (5.2 ± 2) cm/s deduced from QSSPC measurements. The deviation is subject to further analysis. However, in the long-wavelength region of Fig. 7, the improved reflectivity of the PERC structure compared to a full-area Al-BSF is clearly shown. The internal reflectance is increased from 65 % for conventional Al-BSF to 89 % for the rear side passivated PERC solar cell. That leads to an increased IQE in the wavelength regime from 900 nm to 1200 nm and explains the increased J_{sc} of the rear side-passivated solar cell.

4 CONCLUSIONS

The investigated PECVD SiN_y / SiN_x stacks provide an excellent surface passivation before and after a high-temperature firing step with effective surface recombination velocities of (5.2 ± 2) cm/s at $\Delta n = 10^{15}\ cm^{-3}$. We attribute the excellent firing stability to the increased bond strength of hydrogen in the SiN_y

passivation layer compared to pure amorphous silicon as shown in FTIR measurements. Moreover the SiN_x capping layer seems to protect the hydrogen from diffusing out of the SiN_y passivation layer. These assumptions are underlined by hydrogen effusion experiments. We observe a reduced H release due to the presence of nitrogen in the SiN_y network. Our results indicate that the SiN_x capping layer prevents the hydrogen from diffusing out of the SiN_y passivation layer. The application of this novel passivation scheme in large-area screen-printed solar cells results in an energy conversion efficiency of 18.3 % which corresponds to an efficiency improvement of 0.4 % absolute when compared to a reference solar cell with a full-area Al-BSF. However, the rootcause of the relatively high effective rear surface recombination velocity of (400 ± 100) cm/s compared to (5.2 ± 2) cm/s for test wafers with full-area symmetrically passivated surfaces is subject to further analysis.

ACKNOWLEDGMENTS

The authors thank M. Prütz, S. Bräunig, S. Spätlich, and S. Wyczanowski for the sample preparation and J. Schmidt for the fruitful discussions. This work was supported by the German Federal Ministry for the Environment, Nature Conservation and Nuclear Safety under contract No. 0327529A, which is gratefully acknowledged.

REFERENCES

[1] A. W. Blakers, A. Wang, A. M. Milne, J. Zhao, and M. A. Green, Appl. Phys. Lett. 55, 1989, 1363
[2] S. Dauwe, L. Mittelstädt, A. Metz, and R. Hezel, Progr. Photovolt. Res. Appl. 10 (4), 2002, 271
[3] T. Lauinger, J. Schmidt, A. G. Aberle, and R. Hezel, Appl. Phys. Lett. 68, 1996, 115936
[4] A. Upadhyaya, M. Sheoran, and A. Rohatgi, Proceedings 31st IEEE PVSC, 2005, 1273
[5] B. Lenkeit, S. Steckemetz, F. Artuso, and R. Hezel, Energy Materials & Solar Cells 65, 2001, 317
[6] S. Dauwe, J. Schmidt, R. Hezel, Proc. 29th IEEE PVSC, New Orleans, USA, 2002, 162
[7] H. Plagwitz, Y. Takahashi, B. Terheiden, and R. Brendel, Proceedings 21st EUPVSEC, 2006, 688
[8] T. Lauinger, J. Schmidt, A. G. Aberle, and R. Hezel, Appl. Phys. Lett. 68, 1996, 1232
[9] J. Schmidt, J.D. Moschner, J. Henze, S. Dauwe, and R. Hezel, Proceedings 19th EUPVSEC, Paris, France, 2004, 391
[10] P. P. Altermatt, H. Plagwitz, R. Bock, J. Schmidt, R. Brendel, M. J. Kerr, and A. Cuevas, Proceedings 21st EUPVSEC, Dresden, Germany, 2006, 647
[11] H. Plagwitz, PhD thesis at ISFH, Leibniz University Hannover, 2009
[12] A. Ulyashin, D.N. Wright, A. Bentzen, A. Suphellen, E. Marstein, A. Holt, Proceedings 15th Intern. PV SEC, 2007, 1690
[13] S. Gatz, H. Plagwitz, P. P. Altermatt, B. Terheiden, and R. Brendel, Appl. Phys. Lett. 93, 2008, 173502
[14] G. Agostinelli, P. Choulat, H. F. W. Dekkers, E. Vermarien, and G. Beaucarne, Proceedings 4th WCPEC, Waikoloa, USA, 2006, 1004
[15] M. Hofmann, S. Kambor, C. Schmidt, D. Grambole, J. Rentsch, S. W. Glunz, and R. Preu, Advances in OptoElectronics, 2008, 485467
[16] J. Seiffe, L. Gautero, M. Hofmann, J. Rentsch, R. Preu, S. Weber, and R.A. Eichel, J. Appl. Phys. 109, 2011, 034105
[17] H. Mäckel, and R. Lüdemann, J. Appl. Phys. 92, 2002, 2602
[18] S. Dauwe, PhD thesis at ISFH, Leibniz University Hannover, 2004
[19] W. Beyer, Solar Energy Materials & Solar Cells 78, 2003, 235
[20] R. A. Sinton, and A. Cuevas, Appl. Phys. Lett. 69 1996, 2510
[21] H. Nagel, C. Berge, and A. G. Aberle, J. Appl. Phys. 86, 1999, 6218
[22] E. Bustarret, M. Bensouda, M. C. Habrard, J. C. Bruyere, S. Poulin, and S. C. Gujrathi, Phys. Rev. B 38, 1988, 8171
[23] B. Fischer, PhD thesis, University of Konstanz, 2003
[24] P.A. Basore, Proceedings 23rd IEEE PVSC, 1993, 147
[25] R. Brendel, and U. Rau, J. Appl. Phys. 85, 1999, 3634
[26] S. Gatz, K. Bothe, J. Müller, T. Dullweber, and R. Brendel, Energy Procedia Vol. 8, 2011, 318